

Sorption of proteins to charged microgels: characterizing binding isotherms and driving forces

Cemil Yigit, Nicole Welsch, Matthias Ballauff, and Joachim Dzubiella*

*Soft Matter and Functional Materials, Helmholtz-Zentrum Berlin,
Hahn-Meitner Platz 1, 14109 Berlin, Germany and*

*Department of Physics, Humboldt-University Berlin, Newtonstr. 15, 12489 Berlin, Germany**

We present a set of Langmuir binding models in which electrostatic cooperativity effects to protein sorption is incorporated in the spirit of Guoy-Chapman-Stern models, where the global substrate (microgel) charge state is modified by bound reactants (charged proteins). Application of this approach to lysozyme sorption to oppositely charged core-shell microgels allows us to extract the intrinsic, binding affinity of the protein to the gel, which is salt-concentration independent and mostly hydrophobic in nature. The total binding affinity is found to be mainly electrostatic in nature, changes many orders of magnitude during the sorption process, and is significantly influenced by osmotic deswelling effects. The intrinsic binding affinity is determined to be about $7 k_B T$ for our system. We additionally show that Langmuir binding models and those based on excluded-volume interactions are formally equivalent for low to moderate protein packing, if the nature of the bound state is consistently defined. Having appreciated this, a more quantitative interpretation of binding isotherms in terms of separate physical interactions is possible in future for a wide variety of experimental approaches.

I. INTRODUCTION

Functionalized colloids and nanoparticles play an increasingly prominent role in the development of biomaterials and imminent biotechnological applications, for example, drug delivery, enzyme biocatalysis, or control of gene expression.¹⁻⁹ In particular, multiresponsive hydrogels are of great interest due their biocompatibility, resemblance to biological tissue, and tunable viscoelastic properties.^{1,3-5,10-15} Dispersed in water these colloidal microgels create an enormous surface that may be taken as a model for soft biological interfaces. Hence, protein storage, activity, and uptake properties may be changed by physiological stimuli, such as pH, salt concentration, and temperature. Moreover, colloidal hydrogels qualify for a number of applications, e.g., as drug carrier devices.¹⁶⁻¹⁸ However, the detailed control of functionality requires a quantitative understanding of the underlying physical interactions between microgels and biomolecules in the aqueous environment.

Recent studies have demonstrated that protein sorption to nanoparticles is mostly driven by global, nonspecific electrostatic interactions and more local, probably hydrophobic interactions.^{6,7,12,19-26} The balance between those two is highly system-specific and can be manipulated by chemical functionalization or copolymerization. Charged microgels, for instance, can be used to favor or disfavor the sorption of net-charged proteins, while their osmotic swelling and storage volume can be tuned by pH, salt and charge density^{10,11,25,27} essentially via the Donnan equilibrium.²⁸ However, during the uptake of the charged, polyionic proteins, swelling and Donnan equilibria are typically changing in an interconnected fashion.^{19,24-26} These highly *cooperative* effects render the interpretation of binding isotherms, and thus the separation and quantification of global electrostatic and local hydrophobic contributions to binding, a difficult task.

Moreover, binding affinities in these systems depend on protein load which presents an additional complication when modeling the adsorption isotherm.

Up to now, the modeling of protein uptake has been done often by using the standard Langmuir isotherm,^{29,30} in particular when evaluating protein adsorption as measured by isothermal titration calorimetry (ITC).^{6,7,20,22,23,31} In the standard Langmuir approach, however, protein association with single, independent binding sites is assumed which neglects electrostatic cooperativity effects and volume changes during sorption. Additionally the term 'binding' of proteins to soft polymeric layers and hydrogels is somewhat ill defined, as the system may remain in a fluid-like state where proteins are still mobile on average, albeit slower than in bulk.^{13,32} Consequently the stoichiometry and binding affinities to 'sites' in the gel obtained from Langmuir fitting are not so easy to interpret.

Alternatively, the hydrogel matrix may be viewed as a homogeneously charged background to the mobile proteins where saturation of sorption may set in due to excluded-volume (EV) packing. In recent binding models based on such a view,^{25,33-35} it is typically assumed that proteins can be treated as simple charged hard spheres, i.e., hard polyions. The electrostatic problem can then be tackled by approximative Poisson-Boltzman (PB) 'cell' or 'box' models,³³⁻⁴³ where electrostatic cooperativity and osmotic ion effects to deswelling can be included. So far it has not been attempted, however, to separately treat more specific effects in EV-based binding models such as hydrophobic interactions or restraints of the configurational protein degrees of freedom in the bound state. Also the relation between Langmuir and EV models, if any, is unclear. However, modeling protein adsorption by a meaningful and physically sound isotherm is the prerequisite for a quantitative understanding of the driving forces.

Here we present an in-depth discussion of the isotherms suitable for modeling protein sorption into microgels and soft polymeric layers in general. This discussion will then provide the basis for a detailed investigation of the driving forces of protein binding. We demonstrate that electrostatic cooperativity and the effects of microgel volume changes can be introduced into standard Langmuir models following the spirit of Guoy-Chapman-Stern theory for binding of charged molecules to charged surfaces.^{44–46} We test the performance of the binding models by fitting to binding isotherms obtained previously from ITC of chicken egg white lysozyme sorption onto a negatively charged coreshell microgel.²³ The core-shell particles consist of a polystyrene core onto which a charged poly (N-isopropylacrylamide-co-acrylic acid) (NiPAm) network is attached. Previous characterization of this system shows that it is an ideal model system as it reaches full equilibrium with high binding affinities, and the globular lysozyme maintain its folded state in the microgel with even enhanced activity.²³ We then demonstrate that we can separate out the global electrostatic contribution leading to consistent values for the salt concentration independent binding affinity. Finally we show that EV-based binding models are formally equivalent to the Langmuir approach in the low-packing regime if the bound state is consistently defined. Consequences to the interpretation of Langmuir models are discussed.

II. EXPERIMENTS: MATERIALS AND METHODS

A. Materials

In this study the same batch of microgel dispersion was used as in previous work.²³ In brief, the polystyrene core was synthesized by emulsion polymerization in the first step. After purification of the core particles, the microgel shell, containing 5 mol-% N,N-methylenebisacrylamide (BIS) crosslinkers and 10 mol-% acrylic acid with respect to the amount of NiPAm, was polymerized on the polystyrene core by seed polymerization. After purification the particles were transferred into buffer solution by ultrafiltration against 10 mM MOPS buffer at pH 7.2. In this preparation state the gel is swollen and strongly hydrated with more than 90% volume fraction of water. Dynamic Light Scattering (DLS, Malvern Instruments) was applied to determine the hydrodynamic radius of the polystyrene core to $R_{\text{core}} = 62.2 \pm 0.7$ nm and the radius of the total core-shell microgel to $R \simeq 129$ to 172 nm depending on the solution condition.²³

The ITC experiments were performed using a VP-ITC instrument (Microcal) as described previously.²³ Briefly, a total of 300 ml of lysozyme solution (0.695 mM) was titrated into the sample cell filled with 1.4 ml of buffer-matched microgel dispersion at a $c_m = 8.42 \cdot 10^{-7}$ mM concentration. The pH-value was held constant at pH=7.2. The experiments were performed at 298 and

303 K. The following three buffer systems were used: (i) 10 mM MOPS, 2 mM NaN_3 (7 mM ionic strength); (ii) as (i) with additional 10 mM NaCl (17 mM ionic strength); (iii) as (i) with additional 25 mM NaCl (32 mM ionic strength). The incremental heat changes ΔQ were measured during the course of the titration experiment where the protein solution is stepwise injected into the microgel dispersion. The integrated heat change after each injection was corrected by the heat of dilution.

III. THEORY

A. Basic model

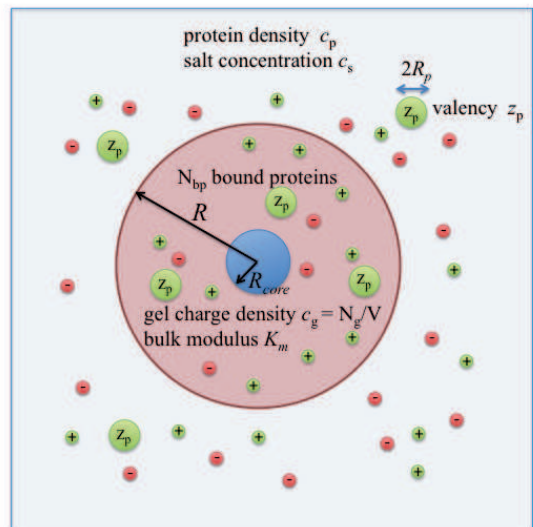


FIG. 1: Illustrative sketch of the model for one core-shell microgel in a protein dispersion. The microgel is represented by a sphere with radius R between 129 and 172 nm including a core with radius $R_{\text{core}} = 62.2$ nm. The gel with volume V has a mean charge density $c_g = N_g/V$. Protein and monovalent salt concentrations in the bulk region are c_p and c_s , respectively. The proteins have radius R_p and valency z_p . N_{bp} is the number of bound proteins.

In our model one core-shell hydrogel particle is modeled as a perfect sphere with radius R having a core with radius R_{core} as depicted in Fig. 1. The net gel volume is therefore $V = 4\pi(R^3 - R_{\text{core}}^3)/3.0$. Potentiometric measurements show that a total number of $N_g = 4.9 \cdot 10^5$ charged monomers are present in the gel. The network monomers are assumed to be homogeneously distributed in the gel as justified by small angle scattering.⁴⁷ The mean gel charge density is $z_g c_g = z_g N_g/V$, where z_g is the monomer charge valency. Since we work at a pH $\simeq 7.2$, much larger than the pK_a -value of $\simeq 4.6$ of polyacrylic acid, and deal with weakly charged gels (with a charge fraction $\simeq 1/10$), we can safely assume that charge regulation plays a minor role and $z_g = -1$ in the follow-

ing. The salt is monovalent with a bulk concentration $c_s = c_+ = c_-$, where c_+ and c_- are the concentrations of cations and anions, respectively. The Bjerrum length is $l_B = e^2/(4\pi\epsilon_0 k_B T)$, where e is the elementary charge, ϵ_0 and $\epsilon(T)$ the vacuum and bulk permittivities, respectively, and $k_B T = \beta^{-1}$ the thermal energy. In our systems $l_B \simeq 0.7$ nm, while the electrostatic Debye-Hückel screening length $\kappa_b^{-1} = (8\pi l_B c_s)^{-1/2}$ in bulk is between $\simeq 3.7$ nm (7 mM salt), $\simeq 2.4$ nm (17 mM salt), and $\simeq 1.7$ nm (32 mM salt).

The lysozyme proteins are modeled by monopolar, homogeneously charged spheres with diameter $\sigma_p = 2R_p$, assumed to have a valency $z_p = +7$ (i.e., a net charge of $+7e$) estimated from titration.⁴⁸ Hence, multipolar contributions, e.g., dipolar or quadropolar or charged-patch interactions to sorption are neglected. The proteins are found in bulk solution with density c_p . No dispersion or other attractive nonelectrostatic interactions between the proteins are considered, and we assume a homogeneous distribution of proteins in the gel region.²³ Aggregation of proteins in the gel is unlikely because at full load the system is still below the solubility threshold of a bulk system at comparable pH and electrolyte concentration.⁴⁹ The number of bound protein inside the gel is denoted by N_{bp} giving rise to an internal protein packing fraction $\eta = N_{bp}\pi\sigma_p^3/6V$. Finally, the gel and the aqueous buffer are modeled as a continuum background with elastic, dielectric, and osmotic properties as detailed in the following sections. The introduced quantities and variables are summarized in Tab.1.

B. Electrostatic contributions to the interactions of the proteins with the charged gel

1. Donnan equilibrium

Homogenization of the charged gel by salt ions leads to a electrostatic potential difference between bulk and gel, the Donnan potential. The latter can be derived by assuming electroneutrality in the gel for monovalent, ideal ions leading to²⁸

$$\Delta\tilde{\phi} \equiv e\beta\Delta\phi = \ln \left[y + \sqrt{y^2 + 1} \right], \quad (1)$$

where $y = z_g c_g / (2c_s)$ is the charge ratio between gel and bulk charge densities and the tilde in $\Delta\tilde{\phi}$ denotes the dimensionless potential scaled by $e\beta$.

We estimate a mean separation of about 2.2 nm between two charged monomers on the same polymer within the gel, considerably larger than the Bjerrum length $l_B \simeq 0.7$ nm. Thus, charge regulation effects by counterion (Manning) condensation or inhomogeneity effects can be safely neglected.⁵⁰⁻⁵³ For our microgel we further estimate the charged monomer concentration to be $c_g = N_g/V \simeq 40-100$ mM, depending on the swelling state. Given bulk salt concentrations between 7 and 32

variable	meaning
R	gel radius
V	gel volume
c_g	charged monomer concentration
c_s	bulk salt concentration
κ_g	inverse Debye length in gel
κ_b	inverse Debye length in bulk
c_p	bulk protein concentration
c_p^{tot}	total protein concentration
x	molar ratio $x = c_p^{\text{tot}}/c_m$
N_{bp}	number of proteins in the gel
N	number of Langmuir binding sites
Θ	protein load $\Theta = N_{bp}/N$
σ_p	effective protein diameter
R_p	effective protein radius
η	protein packing fraction in gel
$\Delta\phi$	Donnan potential
K	binding constant
K_m	gel modulus
constants	meaning
$R_{\text{core}} = 62.2$ nm	core radius
$N_g = 4.9 \cdot 10^5$	number of charged monomers
$z_g = -1$	monomer charge valency
$z_p = 7$	protein charge valency
$c_m = 8.42 \cdot 10^{-10}$ M	microgel concentration
$l_B \simeq 0.7$ nm	Bjerrum length
$v_0 = 1/\text{mol}$	standard volume

TABLE I: Frequently used variables and constants.

mM, thus $|\Delta\tilde{\phi}|$ is on the order of unity ($\simeq 25$ mV) and significant for the interaction with charged macromolecules.

The Donnan equilibrium leads to an osmotic pressure difference π_{ion} between gel and bulk ions and, in the ideal gas limit, is given by the difference of internal and external ionic concentrations²⁸

$$\begin{aligned} \beta\pi_{\text{ion}} &= c_s e^{-\Delta\tilde{\phi}} + c_s e^{\Delta\tilde{\phi}} - 2c_s \\ &= 2c_s \left[\sqrt{y^2 + 1} - 1 \right] = 2c_s [\cosh \Delta\tilde{\phi} - 1]. \end{aligned} \quad (2)$$

For the salts and concentrations considered in this work corrections due to nonideal activity are small⁵⁴ and can be safely neglected.

2. Electrostatic protein-gel interaction

The transfer of a charged protein from the bulk solution with salt concentration c_s into the charged gel with monomer charge concentration c_g is accompanied by a (Gibbs) transfer free energy change per particle (or chemical potential). If we assume the gel monomers to be mobile, this can be modeled by the transfer of a spherical polyion with radius R_p and valency z_p from one bath at salt concentration c_s and zero potential to another at mean potential $\Delta\phi$ and salt concentration c_g . The difference in solvation free energies on a Debye-Hückel level

is then

$$\beta\Delta G_{el} = z_p\Delta\tilde{\phi}(y) - \frac{z_p^2 l_B}{2R_p} \left(\frac{\kappa_g R_p}{1 + \kappa_g R_p} - \frac{\kappa_b R_p}{1 + \kappa_b R_p} \right) \quad (3)$$

where we defined the inverse screening length $\kappa_g = \sqrt{8\pi l_B c_g}$ in the gel, characterizing approximately the screening by mobile polyelectrolyte charges and their neutralizing counterions (see Appendix A). The Donnan potential (1) must now be corrected for the change of total net charge by the charge of bound protein via

$$y = (z_g c_g + z_p N_{bp}/V)/(2c_s). \quad (4)$$

The first, purely entropic term in eq. (3) simply expresses the electrostatic transfer energy of a charge z_p from bulk to a region at potential $\Delta\tilde{\phi}(y)$. The second term reflects the difference in the Born solvation free energies in a salty medium.⁵⁵ The first term is attractive if microgel and protein have opposite net charge, otherwise repulsive, while the second one is attractive if $c_g > c_s$, otherwise repulsive. Since we deal with a weakly charged gel additional entropic effects from the release of condensed counterions can be neglected in our system.⁵⁶

In Appendix A a more rigorous derivation of eq. (3) is presented in the framework of a linearized PB cell model³³⁻⁴³ corrected for particle-particle interactions. While eq. (3) is valid strictly only in the limits of small salt concentrations and small protein charges, its quantitative validity seems to cover a wide range of protein load as long as the protein valency is not too high, as discussed in Appendix A. For our system with lysozyme (surface charge density $\simeq 0.17e/\text{nm}^2$) in monovalent salt and the weakly charged gel (charge fraction 1/10), Debye-Hückel level assumptions are justified.

C. Osmotic and elastic swelling equilibrium

In equilibrium the gel size is determined by a mechanical balance between osmotic and elastic pressures in the gel via^{28,51,57-60}

$$\pi = \pi_{osm} + \pi_{el} = 0. \quad (5)$$

The osmotic term π_{osm} has two contributions one from the solvent, the other from the ions. The first is often expressed by a de Gennes-like scaling type of relation $\propto V^{-n}$, where typically $n = 9/4$ for neutral polymers under good solvent conditions.^{58,61} For charged networks corrections may arise,⁵⁹ while for our case of weakly charged and weakly stretched gels the 9/4 exponent likely to be valid.^{57,58,62} (According to definitions by Dobrynin and Rubinstein,⁵³ we estimate an electrostatic blob size of about 1.3 nm using a monomer length 0.35 nm and our charge fraction 1/10. This is indeed smaller than the correlation length of 3.2 nm given by our mean mesh size, estimated from the linker density.)

The ionic osmotic pressure is dominated by the ideal gas pressure of ions in the gel as given by eq. (2). This is

counterbalanced by the elastic pressure π_{el} as represented essentially by the shear modulus G . Weakly charged networks obey Gaussian chain statistics^{57,59}, and G scales via the power law $\pi_{el} \propto V^{-m}$ with $m = 1/3$. Various experiments corroborate that scaling.^{57,58,62-65} The expression for the total pressure is

$$\begin{aligned} \pi &= AV^{-n} + BV^{-m} + \pi_{ion}(y) \\ &= AV^{-n} \left[1 - \left(\frac{V}{V_0} \right)^{n-m} \right] + \pi_{ion}(y), \end{aligned} \quad (6)$$

where A and B (or V_0) are volume-independent constants. For high salt concentration the ionic contribution vanishes, $\pi_{ion} = 0$, and the equilibrium gel is in the 'neutral' reference state with volume V_0 . The bulk modulus of the gel in this state is defined via $\beta K_m(V_0) = -V\partial\beta P/\partial V|_{T,V_0} = (23/12)A/V_0^n$. By fitting eq. (6) to a variety of salt concentrations (without proteins) we will obtain both the unknowns A and V_0 and thus $K_m(V_0)$.

In first order the effect of protein addition to the gel is lowering of the gel net charge and the inhomogenization of the charge and electrostatic potential distribution inside the gel. As shown in the PB cell model in Appendix A those effects can be approximately included in (6) by replacing $\pi_{ion}(y)$ with

$$\pi_{ion}^p(y) \simeq \pi_{ion}(y) + 2k_B T c_s [\tilde{\phi}(R_c) - \Delta\tilde{\phi}] \sinh(\Delta\tilde{\phi}), \quad (7)$$

with $y = (z_g c_g + z_p N_{bp}/V)/(2c_s)$. The potential $\tilde{\phi}(R_c)$ is the electrostatic potential at the cell boundary R_c in the PB cell model (Appendix A).

Estimating other protein-induced contributions to the pressure from more local effects on elasticity, such as cross-linking by local binding,⁶⁶ conformational restraints of the polymer network, or possible contributions from the protein osmotic pressure is challenging due to the lack of precise knowledge of the nature of the bound state and is out of scope of this paper.

D. Binding isotherms

The transfer of one protein into the gel will be accompanied by a release of the binding enthalpy ΔH . If N_{bp} proteins bind and we assume that the heat per protein does not change with load, the total heat released is

$$Q(N_{bp}) = \Delta H c_m V_{tot} N_{bp}, \quad (8)$$

where V_{tot} is the total titration volume. In the ITC experiments Q is measured vs. the total protein concentration c_p^{tot} . Introducing the molar ratio $x = c_p^{tot}/c_m$ we can write $Q(x) = \Delta H c_m V_{tot} N_{bp}(x)$. The incremental heat $Q'(x) = \partial Q/\partial x$ per molar concentration of protein is more sensitive to fitting and reads

$$Q'(x)/(V_{tot} c_p^{tot}) = \Delta H N'_{bp}(x)/x. \quad (9)$$

For large binding constants and small x , almost all of the proteins immediately get sorbed, and $N_{bp}(x) \simeq x$, and a

plateau of height $Q'(x)/(V_{tot}c_p^{tot}) \simeq \Delta H$ is expected, independent of the binding constant. For large x , typically $N_{bp}(x)$ saturates and $Q'(x) \propto N'_{bp}(x) = 0$. Thus we recognize that fitting to binding models is most sensitive to intermediate values of the molar ratio x , in the pre-saturation regime, near the inflection point of $Q'(x)$.

1. Standard Langmuir Binding Model

The standard Langmuir model is based on identifying the association reaction $A+B \rightarrow AB$, with a binding constant $K = [AB]/[A][B]$, where the square brackets denote concentrations. The basic assumptions in the Langmuir model are that ideal particles are binding to a fixed number N of identical and independent binding sites. The equilibrium constant in the Langmuir framework is usually written as^{29,30}

$$K = \frac{\Theta}{(1 - \Theta)c_p}, \quad (10)$$

where $\Theta = N_{bp}/N$ denotes the fraction of bound protein N_{bp} and total sites N (see also derivation in Appendix B for the canonical ensemble). The protein density outside the gel can be expressed by the total protein density in the sample minus bound protein density by $c_p = c_p^{tot} - N\Theta c_m$. If it is assumed that N , K , and ΔH are protein concentration independent, solving (10) for Θ gives the total heat

$$Q(x) = \frac{1}{2}N\Delta H c_m V_{tot} \left[\xi - \sqrt{\xi^2 - 4x/N} \right], \quad (11)$$

with $\xi = 1 + x/N + 1/(NKc_m)$. The fitting of $Q'(x)/(V_{tot}c_p^{tot})$ to the experimental data then yields the unknown constants K , N , and ΔH . Typically a sigmoidal curve is measured for $Q'(x)$, where ΔH describes the plateau for the first injections (small x), N the inflection point, and K the sharpness of the transition at $x = N$. Fitting to Langmuir isotherms is thus most sensitive close to $x \simeq N$, when the molar ratio equals the number of available binding sites.

The Gibbs binding free energy in the Langmuir model is defined by

$$\beta\Delta G = -\ln(K/v_0), \quad (12)$$

where v_0 is the 'standard volume' which describes the 'effective' configurational volume in one of the binding boxes (see also Appendix B). Thus the absolute value of ΔG depends on the magnitude of the standard volume v_0 , an often overlooked fact in literature.⁶⁷ Typically $v_0 = 1/\text{mol} \simeq 1.6 \text{ nm}^3$ is chosen which is a reasonable choice for molecular binding where spatial fluctuations are on a nanometer length scale. While for quantitative estimates thus precise knowledge of the nature of the bound state is necessary, we will satisfy ourselves in this work with the standard choice $v_0 = 1/\text{mol}$.

2. Extended Langmuir Binding: Separating Nonelectrostatic and Electrostatic Contributions

When many charged entities bind to charged regions a cooperativity effect comes into play due to the change of the global electrostatic properties during loading. This has been appreciated in the Guoy-Chapman-Stern theory for the binding of charged ligands to charged surfaces.⁴⁴⁻⁴⁶ Consequently, the total binding constant $K = K(x)$ has to be defined more generally and split up into an 'intrinsic' part K_0 and an electrostatic part via

$$K(x) = K_0 \exp[-\beta\Delta G_{el}(x)] = \frac{\Theta(x)}{[1 - \Theta(x)]c_p}, \quad (13)$$

i.e., $\Delta G(x) = \Delta G_{el}(x) + \Delta G_0$. In our work we assume $\Delta G_{el}(x)$ to be given by eq. (3). The intrinsic, x -independent binding constant K_0 defines the intrinsic adsorption free energy

$$\beta\Delta G_0 = -\ln(K_0/v_0), \quad (14)$$

which only contains contributions from specific interaction between the protein and the gel environment, and the nonspecific, leading order electrostatic effect has been separated out. Specific interaction may include local solvation effects – where the hydrophobic effect is naturally one of the biggest contributors – and possibly specific local interactions, such as salt bridges.

3. 'Excluded Volume' (EV) Binding Isotherms

An alternative binding isotherm that may be used for evaluating the ITC data is based on the equivalence of chemical potentials in bulk and inside the gel, where in addition to electrostatic and intrinsic binding effects the EV interaction between the (hard spherical) proteins inside the gel are taken into account.^{25,33-35} One assumption is here that in the very contrast to Langmuir models, the proteins are not 'condensed' to fixed sites in the gel but are able to freely move around, under the restraint only that their translational freedom is confined by packing (excluded volume). This ansatz yields the Boltzmann-like equation for the density of hard spheres in the gel

$$N_{bp}/V = \zeta' c_p \exp(-\beta\Delta G_{el} - \beta\Delta G_0) \exp(-\beta\mu_{CS}), \quad (15)$$

where ζ' is the partition function of the bound state more precisely defined later, and μ_{CS} is the Carnahan-Starling (CS) excess chemical potential⁶⁸

$$\beta\mu_{CS} = \frac{8\eta - 9\eta^2 + 3\eta^3}{(1 - \eta)^3} \quad (16)$$

representing the free energy of transferring one hard sphere to a solution with the packing fraction $\eta = (N_{bp}/V)\pi\sigma_p^3/6$. The effective diameter of the sphere

$\sigma_p = 2R_p$ is expected to be close to the diameter of gyration or hydrodynamic diameter of the protein (i.e., $\sigma_p \simeq 3 - 4$ nm for lysozyme)⁶⁹ and will serve as a fitting parameter in the following. Since packing effects play a role in the EV approach we correct the gel volume by the polymer volume fraction. A PNIPAM monomer has an excluded volume roughly of 0.3 nm^3 . We estimate $3.7 \cdot 10^6$ monomers in one microgel what makes $V_{\text{polymer}} \simeq 1.1 \cdot 10^6 \text{ nm}^3$. This corresponds to a polymer volume fraction in the range of 5% (pure, unloaded gel) to 12% (fully loaded gel in 7mM salt).

In (15) we have also separately described the non-specific electrostatic part (ΔG_{el}) and the intrinsic part (ΔG_0) to binding as in the Langmuir model above. In the EV model, the contribution to ΔG_0 can be still thought of being induced by hydrophobic interactions or salt bridges but only in a weak-interaction sense, such that the particles in the gel are still translationally free. However, we additionally consider ζ' in eq. (15), the partition function of the protein in the bound state, which can include contributions from vibrational and orientational restrictions of the protein's degrees of freedom within the gel, e.g., by partial sliding on polyelectrolyte chains.⁷⁰

4. Equivalence Between the Langmuir and the EV Approach

For small protein packing fractions we may linearize the CS chemical potential in eq. (15). We obtain

$$\frac{N_{bp}}{V} \simeq \zeta' c_p \exp(-\beta \Delta G_{el} - \beta \Delta G_0) (1 - 2B_2 N_{bp}/V) \quad (17)$$

where we identified the second virial coefficient of hard spheres $B_2 = 2\pi\sigma_p^3/3$. Physically $2B_2$ describes the volume excluded to the centers of the other spheres taken by one sphere. We rearrange to obtain

$$\exp(-\beta \Delta G_{el} - \beta \Delta G_0) = \frac{N_{bp}/V}{(1 - 2B_2 N_{bp}/V)c_p}. \quad (18)$$

If we now make the substitution $N = V/(2B_2)$ and $\Theta = N_{bp}/N$ as in the Langmuir model above, we end up with the standard Langmuir form (10)

$$\zeta' 2B_2 \exp(-\beta \Delta G_{el} - \beta \Delta G_0) = \frac{\Theta}{(1 - \Theta)c_p}. \quad (19)$$

If $\zeta' = 1$, thus the EV treatment is equivalent to a Langmuir picture where a bound ideal gas particle has a configurational freedom (volume) of $2B_2$, i.e., it can freely move around in one of the N binding boxes. However, as discussed above, in the Langmuir-type bound state the configurations are restricted to an effective configurational volume v_0 with respect to $2B_2$, such that the partition function $\zeta' = v_0/(2B_2)$. With that definition we exactly end up with the standard Langmuir model eq. (10).

Thus, in the approximation of small protein packing $\eta \ll 1$, the EV approach and the standard Langmuir model, eq. (10), are formally equivalent and are allowed to be compared, if $N = V/(2B_2)$ in the Langmuir picture and $\zeta' = v_0/(2B_2)$. The parameter N , the number of fixed binding sites, can then be interpreted as the maximum number of binding spots available for hard spheres simply due to packing in the available volume V . In both models, Langmuir and EV, the binding constant is referenced with respect to a standard volume $v_0 = 1/\text{mol}$.

E. Numerical evaluation including volume change

In the Langmuir approach the derivative $Q'(x) = \partial Q(x)/\partial x$ of eq. (11) is fitted to the experimental data by scanning through ΔH , K_0 , and N values until the least square deviation (LSD) to the experimental data is minimized. The radius R_p is fixed in the Langmuir fittings to 1.8 nm. In the EV approach, eq. (15) is solved numerically and $Q'(x)$, as more generally defined in eq. (9) is fitted to the experimental data by minimizing the LSD. Here the fitting parameters are ΔH , K_0 , and R_p .

One challenge arises because also the gel volume $V = V(x)$ is in general a function of x , the protein concentration. The electrostatic transfer energy defined by eq. (3), in turn, depends on the gel volume. Thus, for separating out the electrostatic contributions to binding, the fitting of binding isotherms needs take into account the volume change. Since a predictive theory for $V(x)$ is out of scope of this paper, we satisfy ourselves in the following by employing experimental DLS data for $R(c_s)$ and $R(x)$ at 7 mM salt concentration as shown in Fig. 2. We fit $V(x) = 4\pi[R(x)^3 - R_{\text{core}}^3]/3$ by the empirical function

$$R(x) = \frac{1}{2}(R_{\text{max}} - R_{\text{min}}) \left[1 - \tanh \frac{x - x_0}{\Delta} \right] + R_{\text{min}}, \quad (20)$$

with R_{max} and R_{min} being the maximum and minimum gel radius at $x = 0$ and $x \rightarrow \infty$, respectively, x_0 is the location of the inflection point, and Δ the distribution width. For $T = 298$ K and 7 mM salt we find $R_{\text{max}} = 172$ nm, $R_{\text{min}} = 129$ nm, $\Delta = 24000$, and x_0 can be identified with $N(7\text{mM})$. For the other salt concentrations, where no DLS data are available, $V(x)$ is obtained by using the known $R_{\text{max}} = 165.7$ nm (17 mM) and 157.1 nm (32 mM) (cf. Fig. 2a) and $x_0 = N$ (cf. Tables II-IV), while $R_{\text{min}} = 129$ nm is used from the 7 mM fit. The now only free variable Δ is employed as an additional parameter obtained by least square fitting the ITC data. We find $\Delta = 31000$ ($c_s = 17$ mM) and 42000 ($c_s = 32$ mM) which appears correlated with the change of the sharpness of the binding isotherms $N_{bp}(x)$ with c_s .

IV. RESULTS AND DISCUSSION

A. Gel shrinking by salt and proteins

In agreement with previous observations,^{10,19,25} DLS shows that the charged PNIPAM microgel shrinks upon the systematic addition of salt as summarized in Fig. 2 (a) up to a concentration of $c_s = 1$ M. The gel radius decreases monotonically and saturates at molar concentrations at a radius close to $R \simeq 139$ nm. The best fit of our mechanical balance approach eq. (6), also shown in Fig. 2 (a), yields very good agreement in almost the whole range of c_s . From the fit we obtain $R(c_s \rightarrow \infty) = R_0 = 138.5$ nm and a bulk modulus $K_m(V_0) = 204$ kPa. Assuming Poisson's ratio to be $1/3$, valid for neutral polyacrylamide or poly-NiPAM gels,^{71,72} then Young's modulus $E \simeq K$. Our determined value for K is thus fully consistent with recently measured Young moduli investigated for varying BIS cross linker density at similar temperatures.⁷³ In the latter E was measured between $\simeq 80$ kPa and $\simeq 500$ kPa for BIS contents of 2% and 10%, respectively, compared to 5% in this work. The good agreement supports our considerations leading to eq. (6).

In Fig. 2(b) we show the measurement of the hydrogel radius $R(x)$ vs. the molar ratio x for the system at 7 mM salt concentration. Analogously to the salt-only case, shrinking of the gel is now observed with increasing protein concentration, i.e., with increasing protein load. At the highest investigated ratio $x \simeq 1.1 \cdot 10^5$ the radius is notably smaller than R_0 pointing to binding-related network tightening. By fitting to the empirical function (20), we find $R_{\min} = 129$ nm. Thus the gel volume under full protein load is $V_0/V_{\min} \simeq 1.3$ times smaller than in the neutral reference state. If we assume that the charged proteins under full load lead to complete charge neutralization and thus $\pi_{ion} \simeq 0$, then the bulk modulus induced by protein binding scales $\propto (V_0/V_{\min})^{9/4}$ and is $\simeq 1.7$ times larger than without proteins, i.e., the gel is roughly 2 times stiffer due to protein sorption. This has to be considered a lower bound as it is likely that ionic contributions to the osmotic pressure still play a role, and maybe protein osmotic effects due to EV interactions need to be considered.

However, in order to check to what amount purely electrostatic effects by proteins induce gel shrinking, we plot the description by eqs. (6) and (7) also in Fig. 2 (b) using the experimental ITC binding isotherm $N_{bp}(x)$ as input. This description is now a prediction and no fitting is involved. While the overall shrinking of the gel is reasonably captured, the model yields a too fast decrease for small x . This may point to shortcomings of the mean-field cell model (Appendix A), where no ion and protein fluctuations are included. For large x , the experimental saturation of $R_{\min} \simeq 129$ nm is not reached indicat-

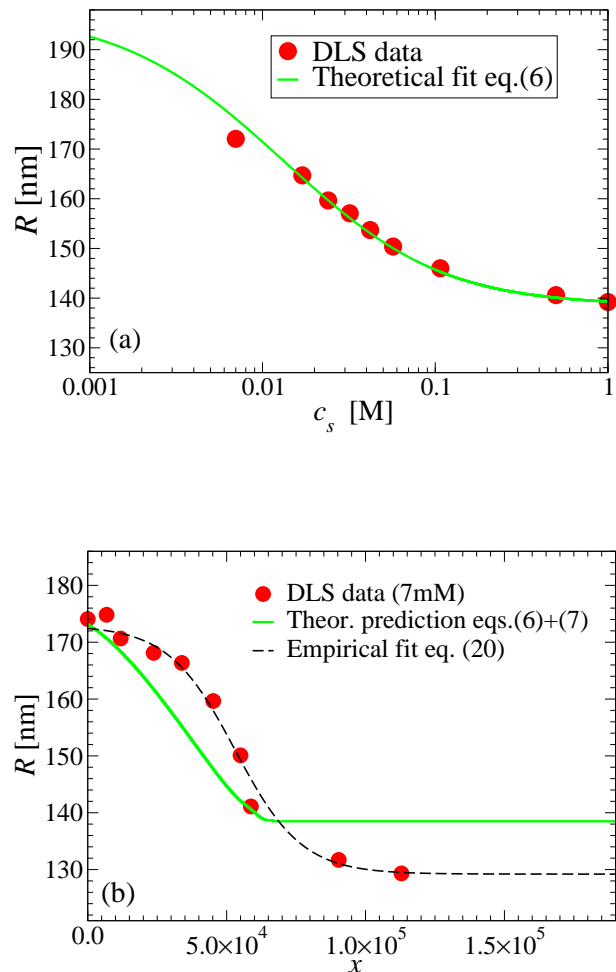


FIG. 2: (a) Microgel radius $R(c_s)$ vs. bulk salt concentration c_s (no proteins). Experimental DLS data (filled circles) are fitted by eq. (6) finding $R_0 = 138.5$ nm and a bulk modulus $K \simeq 204$ kPa. (b) Microgel radius $R(x)$ vs. lysozyme molar ratio $x = c_p^{\text{tot}}/c_m$. The green solid line is the theoretical prediction from eqs. (6) and (7) based on electrostatic considerations only. The dashed line depicts a simple empirical fit to $R(x) = \frac{1}{2}(R_{\max} - R_{\min}) [1 - \tanh \frac{x-x_0}{\Delta}] + R_{\min}$, [eq. (20)] used as input for the fitting of ITC binding isotherms.

ing that nonelectrostatic effects to gel elasticity play a role. Similar unsatisfying performances of simple Donnan models have been observed also in a recent work.²⁵ However, from our comparison it is quite reasonable to judge that the dominant effect to gel shrinking by protein uptake is of ion osmotic origin.

B. Characterizing experimental binding isotherms

1. Langmuir models

The evaluation of the ITC data by the Langmuir-type binding models is presented in Fig. 3 (a). First we compare the results of different model assumptions for 7 mM

ionic strength: i) standard Langmuir model vs. ii) extended Langmuir (including electrostatic cooperativity) with constant volume vs. iii) extended Langmuir including the DLS-measured volume change. From looking at the fits by eye and judging from the overall least square deviation (LSD) to the ITC data, cf. Tab. II, all fits look comparably well and can only be distinguished in the presaturation region around $x \simeq 5 \cdot 10^4$. As discussed above fitting is most sensitive to this transition region. The fitting parameters are summarized in Tab. II: while the heat of binding $\Delta H \simeq 60$ kJ/mol and total number of binding sites $N \simeq 63000$ are relatively insensitive to the model assumptions, the changes in the binding constant are big. From the standard model $\Delta G \equiv \Delta G_0 = -\beta \ln(K/v_0) = -36.6$ kJ/mol. In the extended model without volume change ii), $\Delta G_0 = -24.5$ kJ/mol., i.e., more than 12 kJ/mol correspond to x -dependent electrostatic contributions. Including the volume change, however, has a considerable effect on the electrostatic contribution which grows by 18 kJ/mol. The latter trend is understood by the fact that the monomer charge density $c_g = N_g/V$ increases with shrinking and the contributions in ΔG_{el} as given by eq. (3) rise. Thus considering volume changes in charged systems is important for quantitative fitting, especially in those systems where deswelling is significant. The value of the intrinsic binding free energy is $\Delta G_0 = -18.3$ kJ/mol for 7 mM ionic strength.

In the next step the extended Langmuir model including volume change has been applied to the other ionic strengths 17 and 32 mM as also shown in Fig. 3(a) and summarized in Tab. II. Note again that the starting gel volumes at $x = 0$ decrease for increasing ionic strengths, see the values for R_{max} in Tab. II. Here we first observe that the number of Langmuir binding sites N decreases with higher ionic strength. The reason is *a priori* unclear as the Langmuir model assumes a fixed number of binding sites independent of ionic strength. We further notice that the heat of adsorption ΔH slightly increases with ionic strength. More importantly, however, ΔG_0 stays fairly independent of c_s . Thus, in contrast to the standard Langmuir model, the nonspecific electrostatic contributions have been consistently separated out and the remaining ΔG_0 becomes salt concentration independent. On average we find $\Delta G_0 \simeq -18$ kJ/mol that might be attributable to hydrophobic interactions or possibly other local binding effects.

2. Excluded Volume model

The fitting of the ITC data by the EV model is presented in Fig. 3 (b). Corresponding fitting parameters ΔH , R_p , and ΔG_0 are summarized in Tab. III. As in the Langmuir models the binding isotherms are described very well by the fits judging from the overall LSD to the

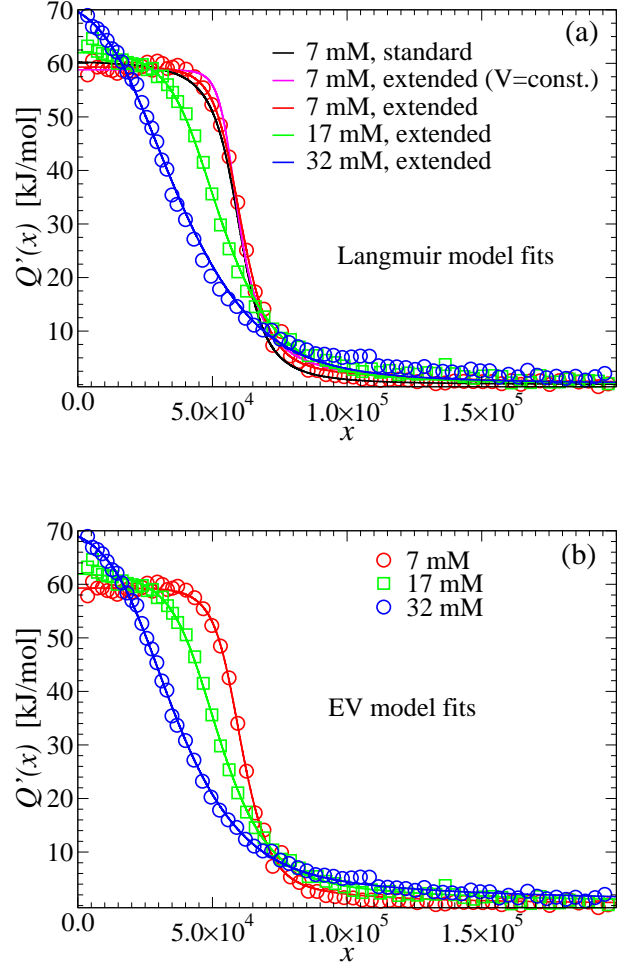


FIG. 3: Fitting of the experimental ITC data (symbols) at 7, 17, 32 mM salt concentrations by different binding models. (a) Langmuir fitting. For 7 mM ionic strength we compare the standard Langmuir description (black line), to the Langmuir model including electrostatic cooperativity with constant gel volume (magenta) and changing gel volume according to eq. (20) (red). The data for 17 (green) and 32 mM (blue) are fitted using the extended model including the volume change. See Table II for obtained fitting parameters. (b) Application of the Excluded Volume (EV) binding model to the same ITC data as in (a). See Table III for obtained fitting parameters.

experimental data. The results for the heat ΔH are also consistent with the Langmuir fits. This is not surprising as this value is determined by the plateau in $Q'(x)$ for small x far away from the saturation regime. The fitting parameter N is now replaced in the EV model by the parameter R_p , the effective hard-core radius of the protein. The analysis yields values of R_p between 1.8 to 2.0 nm, see Tab. III, weakly depending on ionic strength. Those numbers are indeed very close to the hydrodynamic radius of lysozyme of about 1.7 nm.⁶⁹ This good agreement is actually remarkable and justifies the assumptions leading to the EV model, i.e. corroborates well with a packing picture of globular proteins.

c_s [mM]	R_{\max} [nm]	N	ΔH [kJ/mol]	K_0 [l/mol]	ΔG_0 [kJ/mol]	LSD
7 (i)	–	60100	61	$2.6 \cdot 10^6$	-36.6	132
7 (ii)	172.1	65500	59	$1.9 \cdot 10^4$	-24.5	89
7	172.1	63000	59	$1.6 \cdot 10^3$	-18.3	44
17	165.7	57500	62	$2.0 \cdot 10^3$	-18.9	57
32	157.1	42500	72	$1.3 \cdot 10^3$	-17.8	130

TABLE II: Results of fitting to Langmuir models at $T = 298$ K. In the 1st row (i) the results of the standard Langmuir fit without any correction is shown. In the 2nd row (ii) the standard model was corrected for electrostatic cooperativity with a constant gel volume. In rows 3 to 5 the change of gel volume was considered in the fit according to eq. (20). LSD denotes the least square deviation to the experimental data. Lower values correspond to better quality of the fits.

The magnitude of the intrinsic adsorption energy $|\Delta G_0|$ in Tab. III are between 15 and 18 kJ/mol matching closely the ones from the Langmuir model in Tab. II. A very small salt dependence of ΔG_0 remains indicating a slightly less accurate subtraction of the nonspecific effects in this model. However, the salt concentration dependence is quite small and on average we find $\Delta G_0 \simeq -17$ kJ/mol that has to be attributed to specific local binding effects. In Tab. III we also show the results of EV model fitting to experimental data gathered at a higher temperature, $T = 303$ K. The intrinsic binding affinity increases slightly to an average $\Delta G_0 \simeq -18$ kJ/mol which corroborate with the typical thermodynamic signature of increasing hydrophobic association at enhanced temperatures.⁷⁴

c_s [mM]	R_{\max} [nm]	R_p [nm]	ΔH [kJ/mol]	ΔG_0 [kJ/mol]	LSD	T [K]
7	172.1	1.77	59	-14.9	30	298
17	165.7	1.83	62	-17.9	33	
32	157.1	2.01	71	-18.4	25	
7	172.1	1.78	70	-15.1	111	303
17	165.7	1.79	70	-18.9	43	
32	157.1	1.85	65	-19.6	75	

TABLE III: Results of fitting to the Excluded Volume (EV) model at $T = 298$ K (top) and $T = 303$ K (bottom). The change of gel volume was considered in the fit according to eq. (20). LSD denotes the least square deviation to the experimental data. Lower values correspond to better quality of the fits.

3. Donnan potentials $\Delta\phi(x)$ and the binding constant $K(x)$

The Donnan potential $\Delta\phi(x)$, the electrostatic binding energy $\Delta G_{el}(x)$, and so the total binding constant $K(x)$ depend on protein load, and thus, in turn, on the molar ratio x . The Donnan potential $\Delta\phi(x)$ as resulting from the fitting to the extended Langmuir model is plotted in

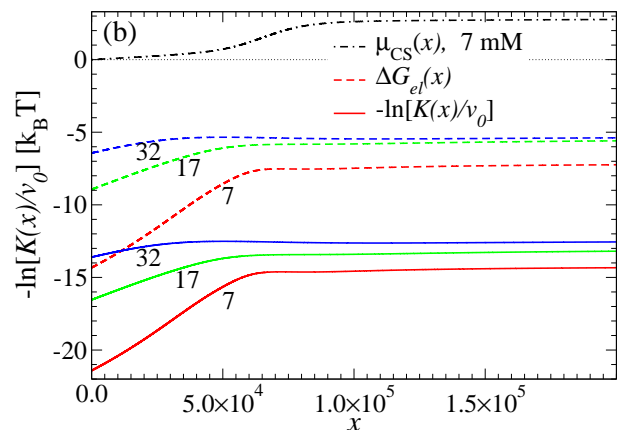
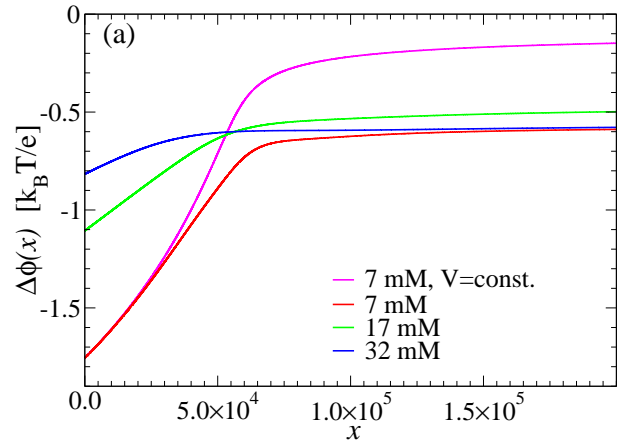


FIG. 4: (a) Mean (Donnan) potential $\Delta\phi(x)$ inside the gel vs. molar ratio x according to the Donnan form eq. (1) and (4) obtained from fitting of the extended Langmuir model to the ITC data. For 7 mM we compare the results from fitting with constant volume vs. variable volume. (b) Total binding affinities $-\ln K(x)/v_0$ (solid lines) and total electrostatic contribution $\Delta G_{el}(x)$ (dashed lines), cf. eq. (3), to the protein transfer energy from the extended Langmuir model for the different ionic strengths 7, 17, 32 mM, as labeled. Also plotted is the hard-sphere Carnahan-Starling contribution μ_{CS} from the EV model fit at 7 mM (dashed-dotted line).

Fig. 4(a) for all ionic strengths. In the case of $c_s = 7$ mM, at the beginning of the titration, $x \simeq 0$, the potential magnitude is a considerable $1.77 k_B T/e$ ($\simeq 44$ mV). The potential quickly decreases with protein load due to charge neutralization, c.f. eq. (4), and saturates for $x \gtrsim N$ due to saturation of $N_{bp}(x)$. The decrease of gel volume in the adsorption process has a notable effect on the potential at large x due to the accompanying increase in monomer charge density. Increasing the ionic strength, on the other hand, considerably lowers the potential at small load, while surprisingly $\Delta\phi$ remains roughly independent of c_s for high load. The reason for the latter

is that less proteins bind for higher ionic strengths, i.e., there is less charge neutralization. The Donnan potential is expected to be highly correlated with the surface potentials of the microgels which govern colloidal stability in solution.²⁵

The total electrostatic contribution $\Delta G_{el}(x)$ to the binding constant is plotted in Fig. 4(b) together with the total binding free energy $-k_B T \ln[K(x)/v_0]$. The curves $\Delta G_{el}(x)$ and $-k_B T \ln[K(x)/v_0]$ are parallel with an offset given by the intrinsic part ΔG_0 , as defined in eq. (13). The electrostatic contribution for very small load ($x = 0$) is big and contributing a favorable $15 k_B T$ ($\simeq 37$ kJ/mol) for 7 mM and $6 k_B T$ ($\simeq 15$ kJ/mol) for 32 mM to the total binding affinity of about $22 k_B T$ and $14 k_B T$, respectively, at the beginning of the titration. We find that the Born contribution (second term in (3)) constitutes a significant (favorable) 2-3 $k_B T$ to the total electrostatic energy and is thus not negligible. All curves decrease in their absolute values and saturate for values $x \gtrsim N$, when the molar ratio exceeds the number of binding sites in the Langmuir model. Note that for 7 mM the saturation value of $K(x)$ is close to the value of K obtained from standard Langmuir fitting, c.f., Tab. II, because fitting is most sensitive to the presaturation region $x \simeq N$ above which $K(x)$ remains constant. This statement holds also for the other salt concentrations when $K(x)$ is compared to previous standard Langmuir fitting.²³

Also shown in Fig. 4 (b) is the Carnahan-Starling contribution μ_{CS} in the EV model. This entropic penalty due to hard sphere packing slowly rises with x in the regime $x \lesssim N$ until quickly increasing to unfavorable $3 k_B T$ in the saturation regime $x \gtrsim N$.

C. Interpretation of Langmuir vs. EV model results

In section IIID 4 we argued that the EV model is equivalent to the Langmuir approach in the low packing regime ($\eta \ll 1$), if N , the number of binding sites, is equated to $V/(2B_2)$ the number of free spots just by packing. Indeed if one now considers a mean gel radius of $R = 150$ nm and protein diameter $\sigma_p = 3.8$ nm obtained from fitting above, we end up with $N = V/(2B_2) \simeq 59000$, totally consistent with numbers obtained from fitting to the Langmuir models above, cf. Table II. This agreement implies that the strict Langmuir assumption of a fixed set of binding sites can still be considered an interpretable quantity, even if the nature of the bound state is ill-defined. From that point of view, the decrease in N in the Langmuir models with increasing ionic strengths can be understood: for increasing c_s , the gel volume V decreases and packing penalties are becoming more important for a smaller number N_{bp} of bound protein. Hence, in standard Langmuir fitting of ITC data for sorption to soft materials,^{6,7,20,22,23,31} where it is likely that not a condensation-like binding of proteins takes place, the stoichiometry of binding may be interpretable by packing

effects.

As we demonstrated in Fig. 4 the electrostatic energies and therefore the binding affinity $K(x)$ are functions of the molar ratio x . How do we interpret a constant K as deduced from standard Langmuir fitting?^{6,7,20,22,23,31} As argued in the Methods section fitting is most sensitive to the presaturation region $x \simeq N$. Indeed the data in Fig. 4 (b) shows that $K(x \simeq N)$ equals the values of standard Langmuir fitting, see Tab. II. Thus, we can conclude that a binding constant obtained from a standard Langmuir fit is a reasonable number which can be interpreted as binding affinities in the presaturation regime, i.e., in the intermediate to high protein load regime, where also volume changes are not so large anymore. However, for small $x \ll N$ (small protein load) our separation into electrostatic and hydrophobic contributions shows that binding affinities can be about 1000 times larger than in the presaturation regime. This may have implications for the modeling and interpretation of protein binding kinetics.^{19,75-77}

It may be on first glance remarkable that in both models, extended Langmuir and EV, the consistent separation of electrostatic and hydrophobic effects yields the same number for the hydrophobic (intrinsic) binding affinity. In our system we find $\Delta G_0 \simeq -7 k_B T$ which must be attributed to nonelectrostatic binding effects and constitutes roughly 1/3 or 1/2 of the total binding affinity in the small and high load regimes, respectively. The very weak dependence of ΔG_0 with salt concentration in both models indicates a successful separation of nonspecific electrostatic and intrinsic effects in our treatment. However, note that the agreement can only be established if the nature of the bound state is identically defined in both models as discussed in section IIID 4. Since at low packing we exemplified total equivalence of both models, the agreement for ΔG_0 is thus not unexpected. Probably for higher packing densities than observed in this study (where $\eta \lesssim 0.18$), the results from both models may disagree stronger. Thus for not too high packing, one model does not seem superior over the other in describing experimentally measured binding isotherms, if correctly interpreted.

Furthermore we would like to comment on the magnitude of $\Delta G_0 \simeq -7 k_B T$ for the intrinsic interaction of lysozyme with the PNIPAM network. If methanemethane interactions are taken as reference with attractions on the order of 2-3 $k_B T$, then 7 $k_B T$ correspond to 2-3 hydrophobic protein-PNIPAM contacts on average which seems reasonable. Increasing temperature led to an increase in ΔG_0 conform with the signature of hydrophobic interactions.⁷⁴ A recent study on a similar system showed hardly uptake of lysozyme by an uncharged PNIPAM microgel.²⁵ Reasons for this discrepancy may be the different gels preparation state, e.g., larger pore sizes within the gel. Alternatively, maybe we overestimate the effects of hydrophobicity and other local effects, such as salt bridges, play a more important role as expected.

Finally, we note that effective net charge of chicken egg white lysozyme as used in this work may be slightly larger on average due to the protonation effects ($z_p \simeq 7$ to 8) within the gel.²³ However, using $z_p = +7.5$ or $+8$ in our analysis we end up with a similar $\Delta G_0 \simeq -7 k_B T$; the reason is that while the prefactor in the electrostatic contribution (3) rises, the Donnan potential (2) decreases quicker with load. These effects roughly cancel each other for our particular system.

V. CONCLUDING REMARKS

In summary we have systematically introduced binding models to characterize the physical interactions in the process of equilibrium protein sorption to microgels. The binding models separate out electrostatic cooperativity and include deswelling effects. The analysis yields a hydrophobic, salt-independent interaction of around $\Delta G_0 \simeq -7 k_B T$ for our core-shell system and hen-egg white lysozyme.

The found ΔG_0 constitutes roughly 1/3 or 1/2 of the total binding affinity in the small and high load regimes, respectively. For small protein load, binding affinities can be about 1000 times larger than in the pre-saturation regime due to high net charge of the protein which is gradually neutralized upon binding. This may have implications for the modeling of protein binding at early stages of sorption, especially to understand kinetic rates.^{19,75–77} Moreover, the Donnan potential is expected to be highly correlated with the surface potentials of the microgels which govern colloidal microgel stability in solution.²⁵

We find gel deswelling to be mostly of electrostatic origin. However, the gel becomes at least 2 times stiffer at high load pointing either to more specific effects at high load (e.g., cross links) or electrostatic correlations not accounted for in mean-field PB cell model approaches. The change and control of material properties upon protein load is essential for functionality,⁵ and suggest challenging investigations in future.

In two complementary models, extended Langmuir and EV, the consistent separation of electrostatic and hydrophobic effects yields the same number for the hydrophobic (intrinsic) binding affinity. The agreement can only be established if the nature of the bound state is identically defined in both models. Details of the bound state can be inferred, for instance, from small angle scattering.⁷⁰ We work at low protein packing; hence, one model does not seem superior over the other in describing experimentally measured binding isotherms, at least for not too high loads (packing). With that a more quantitative interpretation of binding data^{6,7,20,22,23,25,26,31} in terms of separate physical interactions is possible in future. Especially we have shown that fitting based on standard Langmuir models yields interpretable binding affinities and stoichiometry.^{6,7,20,22,23,31} More challenges

arise, however, if the systems of practical interest exhibit microscopic irreversibility and the final protein binding cannot be considered in equilibrium terms.^{9,15}

Acknowledgments

Financial support by the Deutsche Forschungsgemeinschaft (DFG), Schwerpunkt Hydrogele, and by the Helmholtz Virtual Institute is gratefully acknowledged.

Appendix A: Linearized Poisson-Boltzmann (LPB) cell model

To obtain the electrostatic contributions to the transfer of charged hard spheres from bulk to gel we make use of the Poisson-Boltzmann cell model. While often numerical solutions have been employed,^{36–38,40–43,51,78} for weak perturbations the linearized form can be treated analytically.^{33,39}

In the cell model each protein is represented by a homogeneously charged sphere with radius R_p and valency z_p centered in a spherical cell with radius R_c and volume V_c . The gel is assumed to be made up of N_{bp} such cells whose dimensions are determined by the number of proteins in the volume, i.e.,

$$R_c = \left(\frac{3V_c}{4\pi} \right)^{1/3} = \left(\frac{3V}{4\pi N_{bp}} \right)^{1/3} \propto N_{bp}^{-1/3}, \quad (\text{A1})$$

where N_{bp} is the total number of proteins in the volume V . Each cell is in contact with a reservoir with monovalent salt concentration c_s . Inside the gel each cell additionally contains a fixed number of $N_c = N_g/N_{bp}$ charges from the charged network monomers. The mean monomer charge concentration in one cell is thus $N_c/V_c = N_g/V = c_g$. Each cell must be electroneutral on average, i.e., in the gel it holds

$$c_s e^{-\Delta\tilde{\phi}} - c_s e^{\Delta\tilde{\phi}} + z_g c_g + z_p N_{bp}/V = 0, \quad (\text{A2})$$

where we neglected the vanishingly small protein concentration outside of the gel. For high protein load, R_c becomes comparable to R_p and the cell volume needs in principle to be corrected by the protein volume. However, for our systems at highest protein load $(R_p/R_c)^3 \lesssim 0.1$, and the correction is negligible for small and intermediate loads. The solution of (A2) is the modified Donnan potential

$$\Delta\tilde{\phi} = \ln[y + \sqrt{y^2 + 1}] \quad (\text{A3})$$

with $y = (z_g c_g + z_p N_{bp}/V)/(2c_s)$ which describes the difference in the mean electrostatic potential with respect to the bulk reference state where we set $\phi = 0$. In the bulk the protein concentration is typically vanishingly small, thus electroneutrality dictates $c_+ = c_- = c_s$ to a very good approximation.

We now focus on the proteins inside the gel. Here we assume the PE network in the gel to be flexible and fluid-like and thus the N_c charged monomers to behave like mobile counterions to the protein. The PB equation in spherical coordinates is then

$$\frac{1}{r}(r\tilde{\phi})'' = -4\pi l_B[(z_g c \exp(-z_g \tilde{\phi}_1) - c_s \exp(\Delta\tilde{\phi} + \tilde{\phi}_1) + c_s \exp(-\Delta\tilde{\phi} - \tilde{\phi}_1)], \quad (\text{A4})$$

where we made the ansatz $\tilde{\phi}(r) = \Delta\tilde{\phi} + \tilde{\phi}_1(r)$, with $\Delta\tilde{\phi}$ being the constant mean (modified Donnan) potential in eq. (A3) and $\tilde{\phi}_1$ being a perturbation induced by the protein. Note that if the monomers were assumed to be just a fixed, homogeneous background, they would not couple to the field and $c \exp(-z_g \tilde{\phi}_1)$ needed to be replaced by the fixed concentration c_g . The constant c is defined by conservation of the number of monomer charges in the cell via

$$N_c = c \int_{V_c} d^3r \exp(-z_g \tilde{\phi}_1). \quad (\text{A5})$$

It also holds that the average potential equals the Donnan potential, i.e.,

$$\Delta\tilde{\phi} = \frac{1}{V_c} \int_{V_c} d^3r \tilde{\phi}(r) \quad (\text{A6})$$

For not too large protein charges and thus $\tilde{\phi}_1 \ll 1$, we can linearize the exponentials in the PB eq. (A4) with respect to $\tilde{\phi}_1$ which yields

$$\frac{1}{r}(r\tilde{\phi})'' = 4\pi l_B z_p N_{bp}/V + \kappa^2(\tilde{\phi} - \Delta\tilde{\phi}), \quad (\text{A7})$$

where we have identified the internal (gel) charge density $-z_p N_{bp}/V = z_g c_g + c_s \exp(-\Delta\tilde{\phi}) - c_s \exp(\Delta\tilde{\phi})$ from conditions (A5) and (A6), the internal concentration $c_{in} = c_g + c_s \exp(-\Delta\tilde{\phi}) + c_s \exp(\Delta\tilde{\phi})$, and the internal inverse screening length $\kappa = \sqrt{4\pi l_B c_{in}}$. The LPB equation can be solved with respect to the boundary condition that the electrical field on the sphere surface is fixed by $\tilde{\phi}'(R_p) = z_p l_B / R_p^2$ and it vanishes at the cell boundary $\tilde{\phi}'(R_c) = 0$. The final solution is (see also previous works^{33,39})

$$\begin{aligned} \tilde{\phi}(r) &= \Delta\tilde{\phi} + \tilde{\phi}_1(r) \\ &= \Delta\tilde{\phi} - z_p N_{bp}/(V c_{in}) + A \frac{e^{-\kappa r}}{r} + B \frac{e^{\kappa r}}{r} \end{aligned} \quad (\text{A8})$$

with constants

$$A = \frac{z_p l_B e^{\kappa R_p}}{1 + \kappa R_p} \left[1 - e^{-2\kappa(R_c - R_p)} \frac{(\kappa R_p - 1)(\kappa R_c - 1)}{(\kappa R_p + 1)(\kappa R_c + 1)} \right]^{-1}$$

and

$$B = \frac{z_p l_B}{1 + \kappa R_p} \left[e^{\kappa(2R_c - R_p)} \frac{(\kappa R_c - 1)}{(\kappa R_c + 1)} - e^{\kappa R_p} \frac{(\kappa R_p - 1)}{(\kappa R_p + 1)} \right]^{-1}$$

In the limit of large cell sizes, i.e., $R_c \rightarrow \infty$ (or $N_{bp} \rightarrow 0$), it follows that quickly $B \rightarrow 0$, and $A \rightarrow z_p l_B \exp(\kappa R_p)/(1 + \kappa R_p)$. The LPB solution simplifies to

$$\tilde{\phi}(r) = \Delta\tilde{\phi} - z_p N_{bp}/(V c_{in}) + \frac{z_p l_B}{1 + \kappa R_p} \frac{e^{-\kappa(r - R_p)}}{r}. \quad (\text{A9})$$

where we kept the important leading order term in $1/V$. An illustrative sketch of this potential distribution in the cell model is given in Fig. 5. $\Delta\phi$ is the average potential, while for small protein load the potential at the cell boundary $\phi(R_c) \simeq \Delta\tilde{\phi} - z_p N_{bp}/(V c_{in})$ and at the particle surface $\phi(R_p) \simeq \Delta\tilde{\phi} - z_p N_{bp}/(V c_{in}) + (z_p l_B)/[R_p(1 + \kappa R_p)]$. For not too high salt concentrations $c_s \lesssim c_g$, it follows that the Donnan potential $\Delta\phi \gtrsim 1$, and the internal salt concentration can be well represented by $c_{in} \simeq 2c_g$, as the coion concentration ($\propto \exp[-|\Delta\tilde{\phi}|]$) in the gel becomes negligibly small. In the bulk solution in the dilute protein limit analogously to eq. (A9) we find

$$\tilde{\phi}(r) = \frac{z_p l_B}{1 + \kappa_b R_p} \frac{e^{-\kappa_b(r - R_p)}}{r}, \quad (\text{A10})$$

where $\kappa_b = \sqrt{8\pi l_B c_s}$ is the bulk inverse screening length.

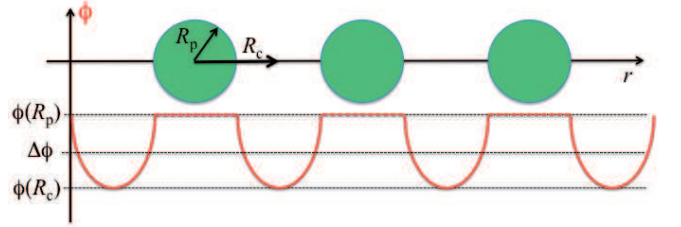


FIG. 5: Illustrative 1D sketch of the electrostatic potential distribution in the cell model: the charged proteins (blue spheres) with radius R_p sit equidistantly in the gel in their cells with radius R_c . $\phi(R_p)$ is the potential at the protein surface, $\phi(R_c)$ the potential at the cell surface, and $\Delta\phi$ the mean (Donnan) potential. In our approach $\phi_1(r)$ is a perturbation of $\phi(r)$ around $\Delta\phi$.

The transfer (Gibbs) free energy (or chemical potential) to bring a protein from bulk solution into the gel can then be calculated by the difference of work of charging the sphere against the surface potential $\phi(R_p)$, $\beta\Delta G = \int_0^{z_p} dz_p [\phi_g(R_p) - \phi_b(R_p)]$ in a cell in the gel (g) vs. bulk (b). We obtain the leading order contributions

(in the low salt and low protein limit)

$$\beta\Delta G_{el} = z_p\Delta\tilde{\phi} - \frac{z_p^2 N_{bp}}{2c_g V} \quad (\text{A11})$$

$$- \frac{z_p^2 l_B}{2R_p} \left(\frac{\kappa_g R_p}{1 + \kappa_g R_p} - \frac{\kappa_b R_p}{1 + \kappa_b R_p} \right),$$

where we defined $\kappa_g = \sqrt{8\pi l_B c_g}$. We did not explicitly integrate over z_p in the second term in (A9) as it is a constant background contribution not immediately involved in the charging process of one particle. It is noteworthy that we obtain the same functional form for ΔG_{el} if the monomer charges are not assumed to be mobile, albeit with a $\sqrt{2}$ smaller internal inverse screening length $\sqrt{4\pi l_B c_g}$ and a factor of 2 in front of the second term.

By a one-to-one comparison of the leading order expression (A11) to the result from employing the full expression (A8) we find that the error in ΔG_{el} is less than $k_B T$ over the whole range of molar ratios and salt concentrations used in this work. By detailed inspection of the behavior of (A9) we observe that the reason of the surprising accuracy is a fortuitous cancellation of errors of higher order terms at large N_{bp} . This fact may shed some doubt on the general applicability of simplified eq. (A11) but note that our parameters (protein valency, salt concentrations, monomer charge densities, etc.) are typical for a wide variety of experimental systems. However, in general the PB approach is expected to break down for very high protein valencies and small proteins, when $|\tilde{\phi}_1| \gg 1$, and strong Coulomb correlations play a role.⁶⁸

The free energy (A11) above considers only ionic contributions to solvation of a fixed lattice of spheres, i.e., it neglects the electrostatic contributions from the interaction between the proteins, i.e., the energy penalty of overlapping double layers. However, in the fluid-like hydrogel protein matrix it is reasonable to assume that proteins can wiggle or move around and are not rigidly fixed to lattice positions. Due to such fluctuations the average surface potential will actually be higher than given in (A8). To estimate the interaction contribution we look at the expansion of the excess chemical potential in terms of virial coefficients, i.e., in first order

$$\beta\mu = 2B_2/V_c, \quad (\text{A12})$$

where $B_2 = -\frac{1}{2} \int d^3r [\exp(-\beta W(r)) - 1]$ and

$$W(r) = W_{HS} + \frac{z_p^2 l_B}{1 + \kappa R_p} \frac{e^{-\kappa(r-R_p)}}{r} \quad (\text{A13})$$

is the protein-protein interaction potential, split up into hard-sphere and the Debye-Hückel contribution according to (A8). Using condition (A6), linearizing the exponent in the defining equation for B_2 , and splitting the chemical potential into hard-sphere and electrostatic contributions we find

$$\beta\mu = \beta\mu_{HS} + \frac{z_p^2 N_{bp}}{2c_g V}. \quad (\text{A14})$$

Thus in leading order the electrostatic protein-protein interaction contribution exactly cancels the second term in (A11) and we end up with the final result for the electrostatic transfer free energy

$$\beta\Delta G_{el} = z_p\Delta\tilde{\phi} - \frac{z_p^2 l_B}{2R_p} \left(\frac{\kappa_g R_p}{1 + \kappa_g R_p} - \frac{\kappa_b R_p}{1 + \kappa_b R_p} \right) \quad (\text{A15})$$

It is interesting to note on the simplicity of eq. (A15) which describes naively the transfer of charge z_p into the average potential $\tilde{\Delta}\phi$ and, in the second term, the difference in Born solvation free energies in a homogeneous medium with salt concentrations c_s and c_g . Thus, the inhomogeneities introduced by the cell model assumption as depicted in Fig. 5 cancel out (in linearized theory) if particle fluctuations are allowed, and the naive form (A15) holds.

The estimation of ionic osmotic contribution to pressure in the presence of proteins seems less simple. Micro-configuration of proteins induce inhomogeneities and the pressure is not anymore given by the simple expression for π in eq. (2). The ion contribution to the osmotic pressure is usually estimated from the ionic concentration at the cell surface (in the cell model) where the electrostatic pressure vanishes,^{33-35,38,39,78}

$$\pi_{ion}^p \simeq c_s \exp(\tilde{\phi}(R_c)) + c_s \exp(-\tilde{\phi}(R_c)) - 2c_s. \quad (\text{A16})$$

Expanding to 1st order in ϕ_1 , we obtain

$$\pi_{ion}^p \simeq \pi_{ion} + 2c_s \tilde{\phi}_1(R_c) \sinh(\Delta\tilde{\phi}), \quad (\text{A17})$$

which recovers $\pi_{ion}^p \simeq \pi_{ion}$ in the limit for vanishing protein concentrations and $\Delta\tilde{\phi}(y)$ is the protein-corrected Donnan potential (A3) with $y = (z_g c_g + z_p N_{bp}/V)/(2c_s)$. Note that this expression does not consider fluctuations in protein positions which is likely to be an important effect to consider in future studies.

Appendix B: The standard Langmuir model in the canonical ensemble

Consider a finite region in space with N identical and independent binding sites available. We denote the number of bound proteins by N_{bp} and define the fraction of bound particles by $\Theta = N_{bp}/N$. The number of available binding states is then^{29,30}

$$W = \frac{\zeta^{N_{bp}} N!}{N_{bp}!(N - N_{bp})!}, \quad (\text{B1})$$

from the combinatorial possibilities of distributing N_{bp} indistinguishable particles on N sites, and ζ is the partition sum of a single particle in the bound state. The Boltzmann entropy is defined by

$$\frac{S}{k_B} = \ln W \quad (\text{B2})$$

leading (within a constant) to the entropy per binding site

$$\frac{S}{Nk_B} = -\Theta \ln \Theta - (1 - \Theta) \ln(1 - \Theta) + \Theta \ln(v_0/\Lambda^3) \quad (\text{B3})$$

where we defined $\zeta^{N_{bp}} = (v_0/\Lambda^3)^{N_{bp}}$ in terms of an effective configurational volume v_0 divided by the cubed thermal (de Broglie) wavelength Λ^3 . 'Effective' means that also restrictions on vibrational and orientational degrees of freedom are adsorbed in the number v_0 , not purely translational effects if it all. The (canonical) Helmholtz free energy of the system is

$$\beta F = \beta F_{id} - \frac{S}{k_B} + \beta N_{bp} \Delta G, \quad (\text{B4})$$

where we introduced the canonical ideal gas free energy $\beta F_{id} = (n - N_{bp})[\ln((n - N_{bp})\Lambda^3/V) - 1]$ with total particle number n . Then $(n - N_{bp})/V$ is the density of unbound particles in a total volume V (assumed to be much larger than the binding region), and the adsorption free energy ΔG associated with the binding of one protein to one Langmuir site. The free energy $\tilde{f} = \beta F/N$ per

binding site is then

$$\begin{aligned} \tilde{f} &= \frac{1}{N}(n - N_{bp})[\ln((n - N_{bp})\Lambda^3/V) - 1] \quad (\text{B5}) \\ &+ \Theta \ln \Theta + (1 - \Theta) \ln(1 - \Theta) \\ &- \Theta \ln(v_0/\Lambda^3) + \beta \Theta \Delta G. \end{aligned}$$

The minimization of the free energy with respect to the number of bound protein $\partial \tilde{f} / \partial N_{bp} = 0$ yields then the final relations for the fraction of bound particles in dependence of the (unbound) particle concentration $c_p = (n - N_{bp})/V$. We obtain the final result

$$K = \exp(-\beta \Delta G) v_0 = \frac{\Theta}{(1 - \Theta) c_p}. \quad (\text{B6})$$

The standard volume v_0 depends on the exact nature of the bound state and is typically not known. Thus the prediction of absolute binding free energies is difficult. In literature often the standard volume $1/\text{mol} \simeq 1.6 \text{ nm}^3$ is employed. This is not unreasonable if one assumes that still rotational and vibrational modes in the bound state take place on molecular, i.e., nanometer scales.

* To whom correspondence should be addressed. E-mail: joachim.dzubiella@helmholtz-berlin.de

- ¹ N. A. Peppas, P. Bures, W. Leobandung, and H. Ichikawa, *Eur. J. Pharm. Biopharm.* **50**, 27 (2000).
- ² F. Caruso, *Advanced Materials* **13**, 11 (2001).
- ³ C. D. H. Alarcon, S. Pennadam, and C. Alexander, *Chem. Soc. Rev.* **34**, 276 (2005).
- ⁴ A. K. Bajpai, S. K. Shukla, S. Bhanu, and S. Kankane, *Prog. Polym. Sci.* **33**, 1088 (2008).
- ⁵ I. Levental, P. C. Georges, and P. A. Janmey, *Soft Matter* **2**, 1 (2006).
- ⁶ T. Cedervall, I. Lynch, S. Lindman, T. Berggard, E. Thulin, H. Nilsson, K. A. Dawson, and S. Linse, *Proc. Natl. Acad. Sci.* **104**, 2050 (2007).
- ⁷ S. Lindman, I. Lynch, E. Thulin, H. Nilsson, K. A. Dawson, and S. Linse, *Nano Letters* **7**, 914 (2007).
- ⁸ M. Calderón, M. A. Quadir, S. K. Sharma, and R. Haag, *Advanced Materials* **22**, 190 (2010).
- ⁹ D. Walczyk, F. B. Bombelli, M. P. Monopoli, I. Lynch, and K. A. Dawson, *J. Am. Chem. Soc.* **132**, 5761 (2010).
- ¹⁰ G. M. Eichenbaum, P. F. Kiser, A. V. Dobrynin, S. A. Simon, and D. Needham, *Macromolecules* **32**, 4867 (1999).
- ¹¹ G. M. Eichenbaum, P. F. Kiser, D. Shah, S. A. Simon, and D. Needham, *Macromolecules* **32**, 8996 (1999).
- ¹² A. P. Sassi, A. J. Shaw, S. M. Han, H. W. Blanch, and J. M. Prausnitz, *Polymer* **37**, 2151 (1996).
- ¹³ C. Khoury, T. Adalsteinsson, B. Johnson, W. C. Crone, and D. J. Beebe, *Biomedical Devices* **5**, 35 (2003).
- ¹⁴ A. W. Bridges, N. Singh, K. L. Burnsa, J. E. Babensee, L. A. Lyon, and A. J. Garcia, *Biomaterials* **29**, 4605 (2008).
- ¹⁵ T. Cedervall, I. Lynch, M. Foy, T. Berggard, S. C. Donnelly, G. Cagney, S. Linse, and K. A. Dawson, *Angewandte Chemie (Intern. Ed.)* **46**, 7574 (2007).
- ¹⁶ W. H. Blackburn, E. B. Dickerson, M. H. Smith, J. F.

- McDonald, and L. A. Lyon, *Bioconjugate Chem.* **20**, 960 (2009).
- ¹⁷ M. H. Smith and L. A. Lyon, *Acc. Chem. Res.* **45**, 985 (2012).
- ¹⁸ S. V. Ghugare, P. Mozetic, and G. Paradossi, *Biomacromolecules* **10**, 1589 (2009).
- ¹⁹ V. A. Kabanov, V. B. Skobeleva, V. B. Rogacheva, and A. B. Zezin, *J. Phys. Chem. B* **108**, 1485 (2004).
- ²⁰ M. De, C.-C. You, S. Srivastava, and V. M. Rotello, *J. Am. Chem. Soc.* **129**, 10747 (2007).
- ²¹ C. Cai, U. Bakowsky, E. Rytting, A. K. Schaper, and T. Kissel, *Europ. J. Pharm. Biopharm.* **69**, 31 (2008).
- ²² T. Jung, W. Kamm, A. Breitenbach, G. Klebe, and T. Kissel, *Pharm. Research* **19**, 1105 (2002).
- ²³ N. Welsch, A. L. Becker, J. Dzubiella, and M. Ballauff, *Soft Matter* **8**, 1428 (2012).
- ²⁴ C. Johansson, P. Hansson, and M. Malmsten, *J. Coll. Interf. Sci.* **316**, 350 (2007).
- ²⁵ C. Johansson, J. Gernandt, M. Bradley, B. Vincent, and P. Hansson, *J. Coll. Interf. Sci.* **347**, 241 (2010).
- ²⁶ Y. Li, R. de Vries, M. Kleijn, T. Slaghek, J. Timmermans, M. C. Stuart, and W. Norde, *Biomacromolecules* **11**, 1754 (2010).
- ²⁷ G. S. Longo, M. O. de la Cruz, and I. Szleifer, *Soft Matter* **8**, 1344 (2012).
- ²⁸ P. J. Flory, *Principles of Polymer Chemistry* (Cornell University Press, Ithaca, NY, 1953).
- ²⁹ M. A. Volmer and P. Mahnert, *Z. Physik. Chem.* **115**, 253 (1925).
- ³⁰ R. I. Masel, *Principles of Adsorption and Reaction on Solid Surfaces* (Wiley Interscience, New York, 1996).
- ³¹ J. B. T. Wiseman, S. Williston and L. Lin, *Anal. Biochem.* **179**, 131 (1989).
- ³² Y. Li, R. de Vries, M. Kleijn, T. Slaghek, J. Timmermans,

- M. C. Stuart, and W. Norde, *Soft Matter* **7**, 1926 (2011).
- ³³ P. M. Biesheuvel and A. Wittemann, *J. Phys. Chem. B* **109**, 4209 (2005).
- ³⁴ W. M. de Vos, P. M. Biesheuvel, A. de Keizer, J. M. Kleijn, and M. A. C. Stuart, *Langmuir* **24**, 6575 (2008).
- ³⁵ P. M. Biesheuvel, F. A. M. Leermakers, and M. A. C. Stuart, *Phys. Rev. E* **73**, 011802 (2006).
- ³⁶ G. Gunnarsson, B. Jönsson, and H. Wennerström, *J. Phys. Chem. B* **84**, 3114 (1980).
- ³⁷ B. Jönsson and H. Wennerström, *J. Phys. Chem. B* **91**, 338 (1987).
- ³⁸ S. Alexander, P. M. Chaikin, P. Grant, G. J. Morales, and P. Pincus, *J. Chem. Phys.* **80**, 5776 (1984).
- ³⁹ A. R. Denton, *J. Phys.: Condens. Matter* **22**, 364108 (2010).
- ⁴⁰ M. N. Tamashiro, Y. Levin, and M. C. Barbosa, *Eur. Phys. J. B* **1**, 337 (1998).
- ⁴¹ M. Deserno, C. Holm, and S. May, *Macromolecules* **33**, 199 (2000).
- ⁴² R. J. Allen and P. B. Warren, *Langmuir* **20**, 1997 (2004).
- ⁴³ P. Hansson, *J. Coll. Interf. Sci.* **332**, 183 (2009).
- ⁴⁴ R. Aveyard and R. Haydon, *Introduction to the Principles of Surface Chemistry*. (Cambridge University Press, Cambridge, 1973).
- ⁴⁵ J. Seelig, *Biochimica et Biophysica Acta-Biomembranes* **1666**, 40 (2004).
- ⁴⁶ S. McLaughlin, *Annu. Rev. Biophys. Biophys. Chem* **18**, 113 (1989).
- ⁴⁷ S. Seelenmeyer, I. Deike, S. Rosenfeldt, C. Norhausen, N. Dingenouts, M. Ballauff, T. Narayanan, and P. Lindner, *J. Chem. Phys.* **114**, 10471 (2001).
- ⁴⁸ D. E. Kuehner, J. Engmann, F. Fergg, M. Wernick, H. W. Blanch, and J. M. Prausnitz, *J. Phys. Chem. B* **103**, 1368 (1999).
- ⁴⁹ P. Retailleau, M. Riés-Kautt, and A. Ducruix, *Biophys. J.* **73**, 2156 (1997).
- ⁵⁰ D. I. Devore and G. S. Manning, *Biophys. Chem.* **2**, 42 (1978).
- ⁵¹ M. D. Buschmann and A. J. Grodzinsky, *J. Biomechanical Eng.* **117**, 179 (1995).
- ⁵² K. B. Zeldovich and A. R. Khokhlov, *Macromolecules* **32**, 3488 (1999).
- ⁵³ A. V. Dobrynin and M. Rubinstein, *Prog. Polym. Sci* **30**, 1049 (2005).
- ⁵⁴ R. A. Robinson and R. H. Stokes, *Electrolyte Solutions* (Dover Publications, New York, 2002).
- ⁵⁵ D. A. McQuarrie, *Statistical Mechanics* (University Science Books, Sausalito, California, 2000).
- ⁵⁶ K. Henzler, B. Haupt, A. Wittemann, O. Borisov, and M. Ballauff, *J. Am. Chem. Soc.* **132**, 3159 (2010).
- ⁵⁷ S. A. Dubrovskii, G. V. Rakova, M. A. Lagutina, and K. S. Kazanskii, *Polymer* **42**, 8075 (2001).
- ⁵⁸ F. Horkay and M. Zrinyi, *Macromolecules* **15**, 1306 (1982).
- ⁵⁹ M. Rubinstein, R. H. Colby, A. V. Dobrynin, and J.-F. Joanny, *Macromolecules* **29**, 398 (1996).
- ⁶⁰ J. T. G. Overbeek, *Prog. Biophys. Biophys. Chem.* **6**, 58 (1956).
- ⁶¹ P. G. de Gennes, *Scaling concepts in Polymer Physics* (Cornell University Press, Ithaca, NY, 1979).
- ⁶² Z. Hu, C. Li, and Y. Li, *J. Chem. Phys.* **99**, 7108 (1993).
- ⁶³ R. Skouri, F. Schosseler, J. P. Munch, and S. J. Candau, *Macromolecules* **28**, 197 (1995).
- ⁶⁴ G. Nisato, R. Skouri, F. Schosseler, J.-P. Munch, and S. Candau, *Faraday. Discuss.* **101**, 133 (1995).
- ⁶⁵ S. A. Dubrovskii and G. V. Rakova, *Macromolecules* **30**, 7478 (1997).
- ⁶⁶ R. Borrega, C. Tribet, and R. Audebert, *Macromolecules* **32**, 7798 (1999).
- ⁶⁷ H.-X. Zhou and M. K. Gilson, *Chem. Rev.* **109**, 4092 (2009).
- ⁶⁸ J.-P. Hansen and I. McDonald, *Theory of Simple Liquids* (Academic Press, London, 2006).
- ⁶⁹ A. C. Hamill, S. C. Wang, and C. T. Lee Jr., *Biochemistry* **44**, 15139 (2005).
- ⁷⁰ K. Henzler, S. Rosenfeldt, A. Wittemann, L. Harnau, S. Finet, T. Narayanan, and M. Ballauff, *Phys. Rev. Lett.* **100**, 158301 (2008).
- ⁷¹ Y. Li, Z. Hu, and C. Li, *J. Appl. Pol. Sci.* **50**, 1107 (1993).
- ⁷² J. Yoon, S. Cai, Z. Suo, and R. C. Hayward, *Soft Matter* **6**, 6004 (2012).
- ⁷³ A. Burmistrova, M. Richter, C. Uzum, and R. von Klitzing, *Coll. Pol. Sci.* **289**, 613 (2011).
- ⁷⁴ K. A. Dill and S. Bromberg, *Statistical Thermodynamics in Chemistry and Biology* (Garland Science, New York and London, 2003).
- ⁷⁵ D. Dell'Orco, M. Lundqvist, C. Oslakovic, T. Cedervall, and S. Linse, *Plos One* **5**, e10949 (2010).
- ⁷⁶ E. Casals, T. Pfaller, A. Duschl, G. J. Oostingh, and V. Puntès, *ACS Nano* **4**, 3623 (2010).
- ⁷⁷ N. Welsch, , J. Dzubiella, and M. Ballauff, *Soft Matter* (2012), submitted.
- ⁷⁸ R. A. Marcus, *J. Chem. Phys.* **23**, 1057 (1955).

FIG. 6: TOC figure

